SUPPLEMENTAL INFORMATION

Fibrotic venous remodeling and non-maturation of arteriovenous fistulas

Laisel Martinez, PharmD[1], Juan C. Duque, MD[2], Marwan Tabbara, MD[1], Angela Paez, MD[1], Guillermo Selman, PhD[1], Diana R. Hernandez, PhD[1], Chad A. Sundberg[3], Jason Chieh Sheng Tey[3], Yan-Ting Shiu, PhD[3], Alfred K. Cheung, MD[3-5], Michael Allon, MD[6], Omaida C. Velazquez, MD[1], Loay H. Salman, MD[7], Roberto I. Vazquez-Padron, PhD[1,*]

[1]DeWitt Daughtry Family Department of Surgery, Leonard M. Miller School of Medicine, University of Miami, Miami, FL; [2]Department of Medicine, Leonard M. Miller School of Medicine, University of Miami, Miami, FL; [3]Division of Nephrology and Hypertension, University of Utah, Salt Lake City, UT; [4]Medical Service, Veterans Affairs Salt Lake City Healthcare System, Salt Lake City, UT; [5]Department of Nephrology, The Second Xiangya Hospital, Central South University, Changsha, Hunan, China; [6]Division of Nephrology, University of Alabama at Birmingham, Birmingham, AL; [7]Division of Nephrology and Hypertension, Albany Medical College, Albany, NY

***Corresponding Author:**

Roberto I. Vazquez-Padron, Ph.D.
Division of Vascular Surgery
University of Miami
Miller School of Medicine
1600 NW 10th Ave, RMSB 1048
Miami, FL 33136
rvazquez@med.miami.edu

TABLE OF CONTENTS

SUPPLEMENTARY METHODS

Preoperative Mapping and Surgical Technique

Patients underwent venous and arterial mapping of the upper extremities using Duplex ultrasound. Using a warm environment and a proximal tourniquet, the cephalic, basilic, and brachial veins are imaged in the forearm and arm. The most distal vein that is of good quality (not thickened or compressible) and ≥3.5 mm in diameter is used. We followed the order of AVF preference recommended by the National Kidney Foundation/Kidney Disease Outcomes Quality Initiative.[1] The preferred order per guidelines is: cephalic, basilic, and brachial. The adjacent artery is also evaluated. We used the brachial artery if ≥ 4.0 mm in diameter or the radial artery if ≥ 2.5 mm. If there is any calcification in the radial artery, a wrist fistula is not done even if the cephalic vein is adequate. Our academic center is a tertiary referral center, where most of our patients had previous access placements or do not have adequate forearm veins or arteries, necessitating an upper arm AVF.

All procedures involved monitored anesthesia care (MAC) with generous local anesthesia using 1% lidocaine and 0.25% Marcaine in a 1:1 ratio. The basilic vein or brachial vein was located and transected above the elbow. The first vein biopsy was collected at this time. The vein was flushed with heparinized saline and the entire length of the dilator was passed to make sure there was no obstruction. The size of the dilator was noted and the resultant diameter was used in our calculations as the internal cross-sectional diameter of the vein. An end vein-to-side artery anastomosis was performed using the standard running parachute technique. To create the first-stage anastomosis, the surgeon dissects and ties off the basilic vein entering the arm from the forearm and the medial cubital vein above the elbow. The basilic vein proximal to the above branches or to any large branch was used in order to force all the flow into that vein and avoid

any shunting into the branch. The median anastomosis diameter was 4.5 mm [IQR 4.5-4.5]. The incision was closed only if the radial pulse was maintained and the thrill was easily palpable through the skin. Immediately after anastomosis, the vein was compressed as proximal as possible in the upper arm allowing the increased pressure in the vein to dilate it. If the radial pulse was not palpable, banding of the inflow segment of the vein was performed with either clips or sutures to decrease the caliber to a diameter similar to the artery.

The median time for the second-stage procedure in enrolled patients was 76 days [IQR: 56 – 112]. We evaluated the first stage procedure by physical exam and, if the surgeon felt that the thrill started at the anastomosis and went to the upper arm, the patient was scheduled for the second stage. Duplex ultrasound was done in cases where the physical exam revealed a fistula that did not meet the above criteria, allowing the surgeon to plan for a graft extension. Moreover, if during the second procedure, a significant portion of the AVF was < 6 mm in diameter, then a graft extension was done to the more proximal dilated vein. The transposition was done by transecting the AVF, routing it subcutaneously, and re-anastomosing to the stump on the artery or a new more proximal anastomosis was done. Care was taken not to create the tunnel too lateral in order to avoid a large angle in the proximal arm. If the vein was too short, a new anastomosis was done to the brachial artery proximal to the ligated stump.

Histological and Morphometric Analysis

The native vein and AVF venous samples were 1-2 mm in length and were collected at the site of transection during the first-stage anastomosis surgery and the second-stage transposition procedure. The AVF biopsy was taken approximately 2 cm from the initial

anastomosis, if the length of the transected AVF was long enough to allow its transposition. Vein and AVF biopsies were submerged in neutral formalin immediately after collection, and de-identified and labeled with a numerical code once transferred to the research laboratory. Tissues were paraffin-embedded and sectioned for histology. Tissue sections were stained with Masson's trichrome for gross histopathological analysis. Full digital images were acquired with a Visiontek digital microscope (Sakura, Torrance, CA). Medial fibrosis (% area of collagen) was quantified using ImageJ (National Institutes of Health, Bethesda, MD) and color thresholding methods. Briefly, images were converted to RGB format and color thresholds on the blue channel were used to segment the blue (collagen) from the red/pink (cells) staining. The intima and media areas were delineated to calculate % medial fibrosis and intimal hyperplasia (IH; defined as intima/media area ratio). Change in medial fibrosis and IH over time was calculated by subtracting the pre-existing value from the postoperative measurement in patients from whom both vein and AVF samples were available. Operators blinded to the clinical data performed image digital processing and morphometric measurements.

Second-Harmonic Generation Microscopy and Collagen Fiber Analysis

Standard light microscopy is useful to quantify medial collagen but does not provide information about the organization of the collagen fibers. Non-linear second harmonic generation (SHG) microscopy provides information about the organization (e.g., alignment and orientation) of collagen fiber bundles within the media, as it detects only collagen in fiber bundles and not diffuse collagen molecules.[2] SHG signals of collagen fiber bundles in unstained paraffin-embedded tissue sections (5-μm thickness; 70 veins and 85 AVFs) were acquired at 850 nm excitation under a multi-photon microscope (Prairie Technologies). At least three fields per

sample were acquired, and analyzed for fiber patterns and orientation angles by three independent observers blinded to the patient's clinical characteristics and AVF outcomes. Categorical fiber patterns were assigned as described previously.[3] Algorithms in Fiber Analyzer for anisotropy index and OrientationJ for orientation angle were used for image analysis.[4,5] Anisotropy index is the degree of alignment of the fibers, ranging from "0" for totally random (*i.e.*, no preferential directionality) to "1" for totally aligned in one direction. Each fiber's orientation angle is given as the angle between the fiber's main axis and the perimeter of the adjacent lumen, ranging from 0^{o} (perpendicular to the lumen = radial direction) to 90^{o} (circumferential direction).

Statistical Analysis

Statistical analyses were performed using the XLSTAT software and GraphPad Prism version 5.00 for Windows (GraphPad Software, San Diego, California, USA). Normally distributed data were compared using t-test and expressed as mean ± standard deviation; otherwise, the Mann-Whitney test was used and data expressed as median and IQR. Comparisons of longitudinal samples from the same patient (tissue pairs) were performed using paired t-tests with unequal variances. Associations between clinical covariates (sex, age, diabetes, and history of a previous AVF) and AVF non-maturation were assessed using a stepwise forward logistic regression model with probabilities for entry and removal of 0.15 each. Associations between clinical covariates and vascular features were assessed using multivariate general linear regressions adjusted for sex, age, diabetes, and history of a previous AVF. The association of fibrosis or IH with anatomical AVF non-maturation was determined using univariate logistic regression models or multivariate models adjusted for sex. The associations

between collagen patterns, orientation angle or anisotropy index and AVF non-maturation was evaluated with univariate logistic regressions.

SUPPLEMENTAL RESULTS

Characterization of the Patient Cohort

Table 1 summarizes the demographic, clinical, and vascular access characteristics of the entire patient cohort and the three study subgroups (Veins, AVFs, and Pairs) after the necessary exclusions. The mean age of the patient cohort was 56.0 ± 13.3 years (mean ± standard deviation). The demographic composition consisted of 41% females, 63% non-Hispanic blacks, and 35% Hispanics. Most patients had a history of hypertension (97%), 46% had diabetes, 22% had coronary artery disease, and 8% had congestive heart failure. Sixty-two percent of the study population was taking antiplatelet agents (aspirin and/or clopidogrel), 62% were on statins, and 38% were treated with an angiotensin-converting enzyme inhibitor (ACE-I) or angiotensin II receptor blocker (ARB). Most AVFs used the brachio-basilic configuration (83%), while 11% were brachio-brachial, 4% were brachio-cephalic, and 2% were radial-basilic. The median time interval between first-stage and second-stage surgeries was 76 days (56-112 interquartile range [IQR]). Twenty-one percent of patients had a history of a previous AVF. The three patient subgroups and the full population were similar with respect to the above characteristics, with the exception of a higher proportion of brachio-brachial AVFs in the postoperative and full cohorts.

Clinical Outcomes

Among the 165 patients enrolled in the study, three (1.8%) died, including two prior to the second-stage procedure and one 3 months after the second-stage procedure. One patient (0.6%) developed severe steal syndrome requiring AVF ligation. After excluding four patients due to loss of follow-up (including the two participants who died prior to the second-stage surgery), non-maturation occurred in 39 of 161 AVFs (24%).

REFERENCES

1. National Kidney Foundation: KDOQI Clinical Practice Guideline for Hemodialysis Adequacy: 2015 Update. *Am J Kidney Dis* **66**: 884-930, 2015
2. Chen X, Nadiarynkh O, Plotnikov S, Campagnola PJ: Second harmonic generation microscopy for quantitative analysis of collagen fibrillar structure. *Nat Protoc* **7**: 654-669, 2012
3. Shiu YT, Litovsky SH, Cheung AK, et al.: Preoperative Vascular Medial Fibrosis and Arteriovenous Fistula Development. *Clin J Am Soc Nephrol* **11**: 1615-1623, 2016
4. Sander EA, Barocas VH: Comparison of 2D fiber network orientation measurement methods. *J Biomed Mater Res A* **88**: 322-331, 2009
5. Rezakhaniha R, Agianniotis A, Schrauwen JT, et al.: Experimental investigation of collagen waviness and orientation in the arterial adventitia using confocal laser scanning microscopy. *Biomech Model Mechanobiol* **11**: 461-473, 2012

Supplemental Table 1. Association between baseline covariates and anatomical non-maturation

Covariate[a]	Odds Ratio (OR)	95% Confidence Interval	*P* Value
Age	1.013	0.984 – 1.042	0.39
Female Sex	2.467	1.170 – 5.202	0.018
Diabetes[b]	N/A	N/A	N/A
Previous AVF	2.240	0.953 – 5.264	0.064

[a] *The reference status for binary covariates is male sex, no diabetes, and no history of previous AVF.*
[b] *Covariate removed by a stepwise logistic regression model with probabilities for entry and removal of 0.15 each.*

Supplemental Table 2. Association between collagen deposition patterns and anatomical non-maturation

	Odds Ratio (OR)	95% Confidence Interval	*P* Value
Pre-existing			
MPMP[a]	1.465	0.322 – 6.669	0.62
MPMP or Parallel[b]	4.128	0.477 – 35.72	0.20
Postoperative			
MPMP[a]	0.583	0.152 – 2.237	0.43
MPMP or Parallel[b]	1.312	0.313 – 5.497	0.71

The reference status is non-MPMP ([a]) and patterns other than MPMP or parallel ([b]). Abbreviations: MPMP, micro-perpendicular with macro-parallel.

Supplemental Figure 1

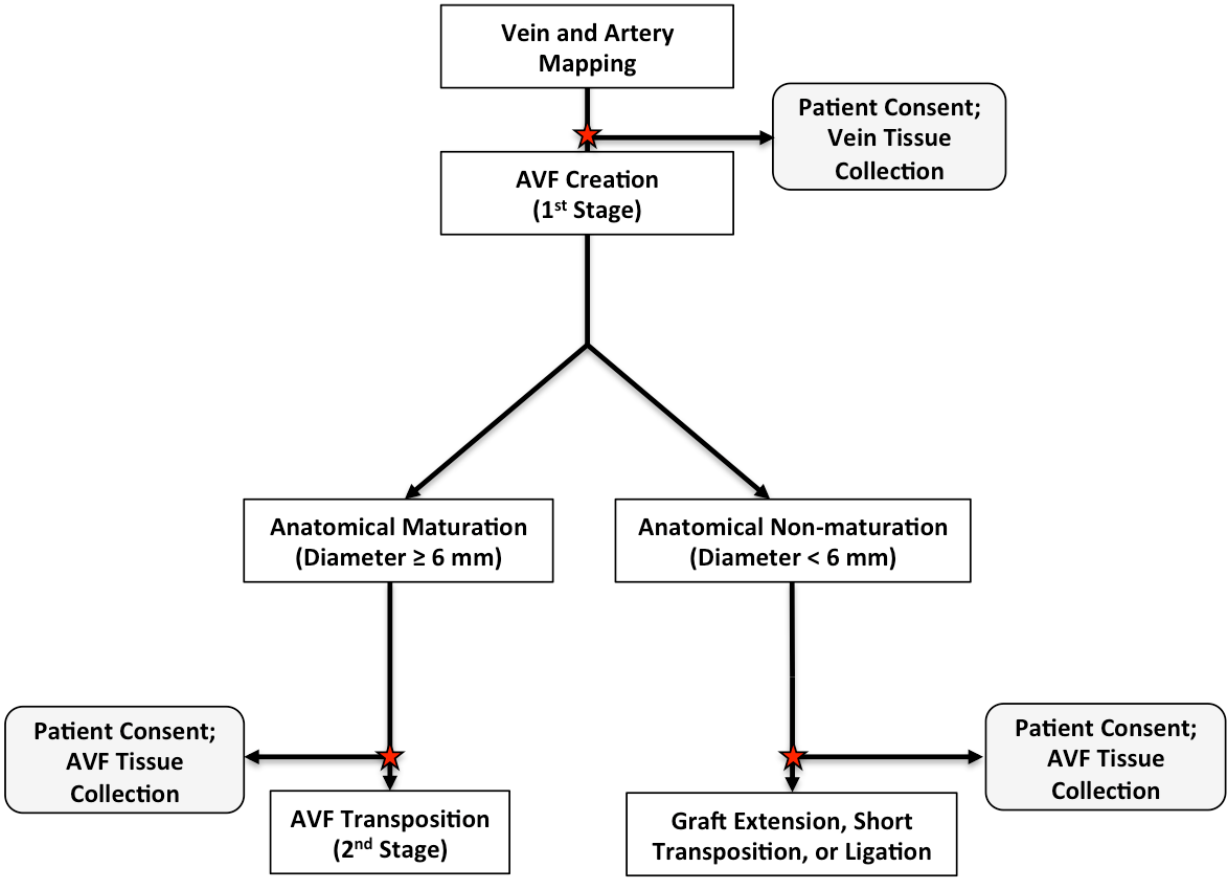

Supplemental Figure 1. Flow diagram of surgical procedures and sample collection. The chart illustrates the flow of surgical procedures performed on mature and failed AVFs, and the times of sample collection. Native vein and AVF venous biopsies were obtained intraoperatively prior to the arteriovenous anastomosis (first-stage surgery) and AVF transposition (second-stage surgery) or salvage procedures.

Supplemental Figure 2

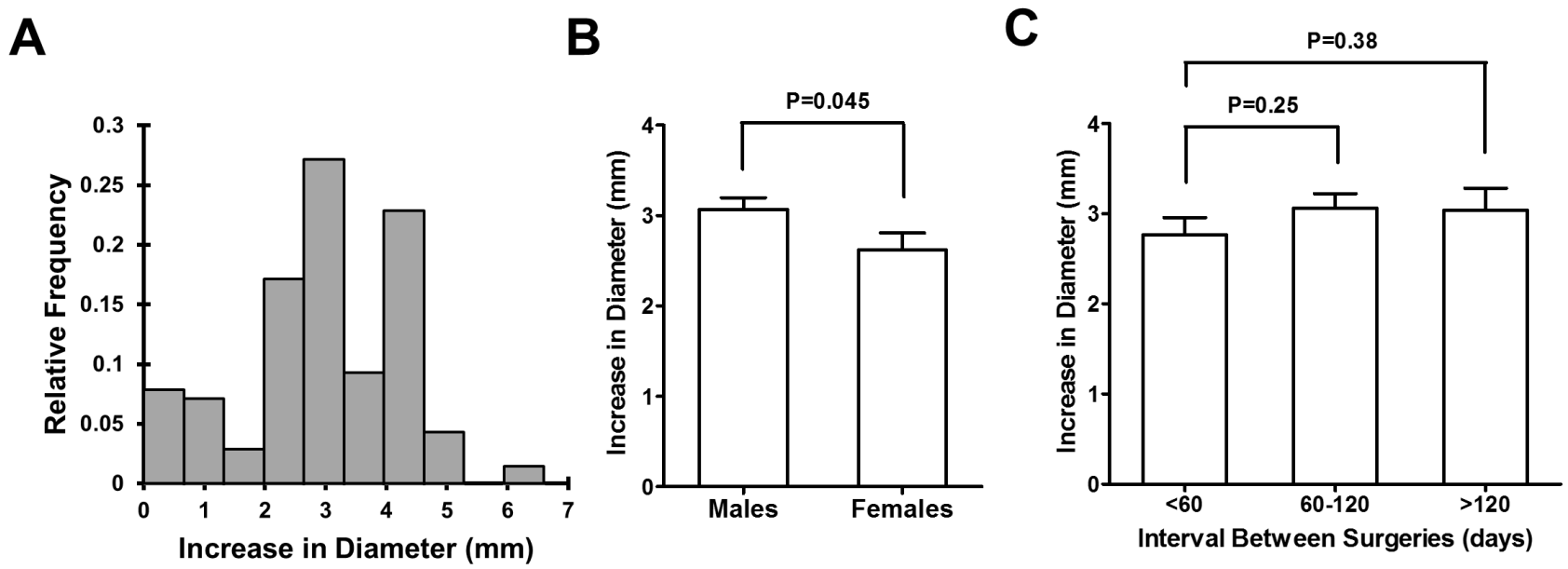

Supplemental Figure 2. Increase in internal vein diameter during maturation. **A)** Distribution of the increase in vein diameter from first-stage to second-stage surgery. Increase in diameter was calculated as the internal cross-sectional diameter of the remodeled AVF minus that of the native vein. **B-C)** Increase in internal vein diameter as determined by patient's sex **(B)** and by the time interval between first-stage and second-stage surgeries **(C)**. Diameter values are presented as mean ± standard error of the mean (SEM).

Supplemental Figure 3

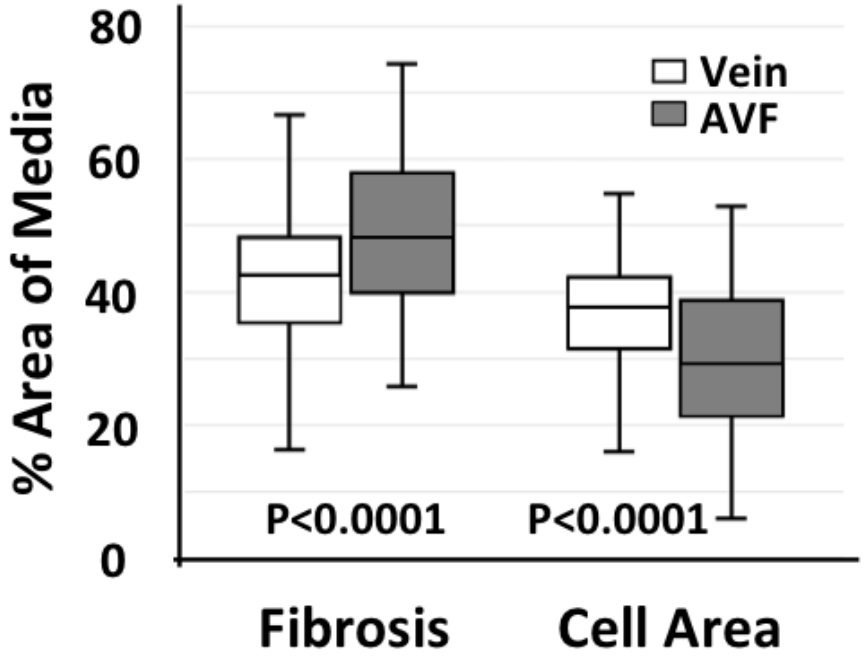

Supplemental Figure 3. Pre-existing and postoperative medial fibrosis. Comparisons of the mean medial fibrosis and cell percent area in native veins and AVFs using the entire first-stage (pre-existing) and second-stage (postoperative) cohorts.

Supplemental Figure 4

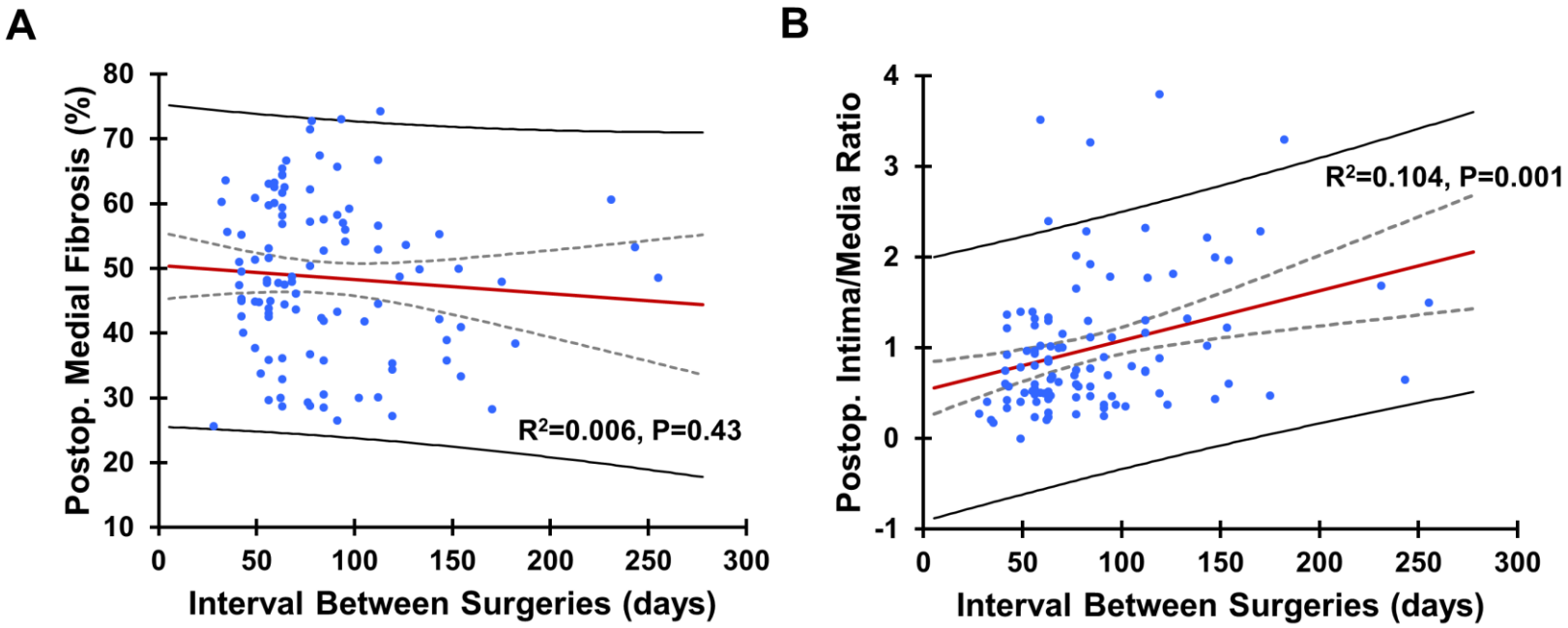

Supplemental Figure 4. Association of medial fibrosis and intimal hyperplasia with time interval between surgeries. Effect of time interval between first-stage and second-stage surgeries on the development of postoperative medial fibrosis **(A)** and intimal hyperplasia **(B)**.

Supplemental Figure 5

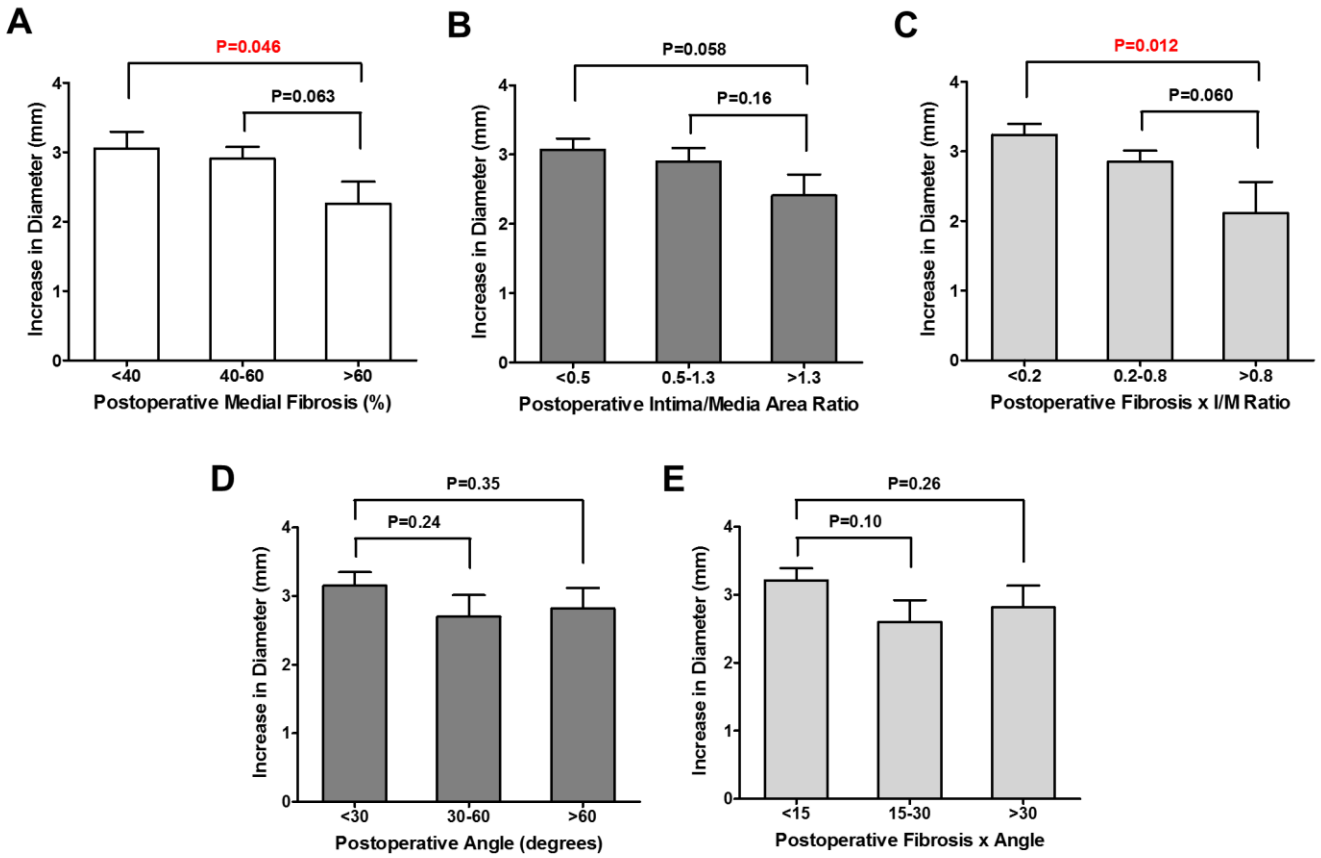

Supplemental Figure 5. Effect of fibrosis, intimal hyperplasia, and collagen angle on the increase in vein diameter. Increase in internal vein diameter during maturation as determined by postoperative medial fibrosis **(A)**, intimal hyperplasia (IH; **B**), the medial fibrosis x IH product **(C)**, collagen orientation angle **(D)**, and the medial fibrosis x angle product **(E)**. Increase in diameter was calculated as the internal cross-sectional diameter of the remodeled AVF minus that of the native vein. Intimal hyperplasia is expressed as the intima/media area ratio. Medial fibrosis is expressed as a decimal in the calculation of products terms. Diameter values are presented as mean ± standard error of the mean (SEM).

Supplemental Figure 6

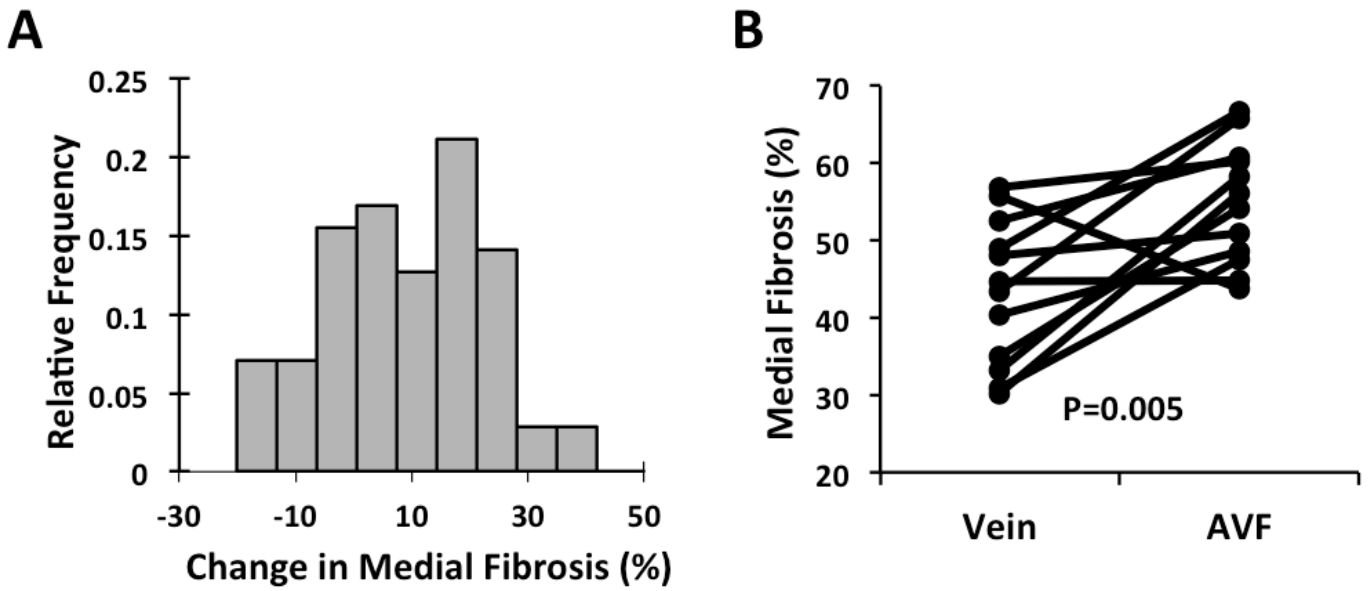

Supplemental Figure 6. Change in medial fibrosis over time in tissue pairs. A) Distribution of longitudinal change in medial fibrosis in patients from whom both the vein and AVF samples were collected (tissue pairs). **B)** Pairwise comparison of medial fibrosis in tissue pairs of patients with anatomical non-maturation.

Supplemental Figure 7

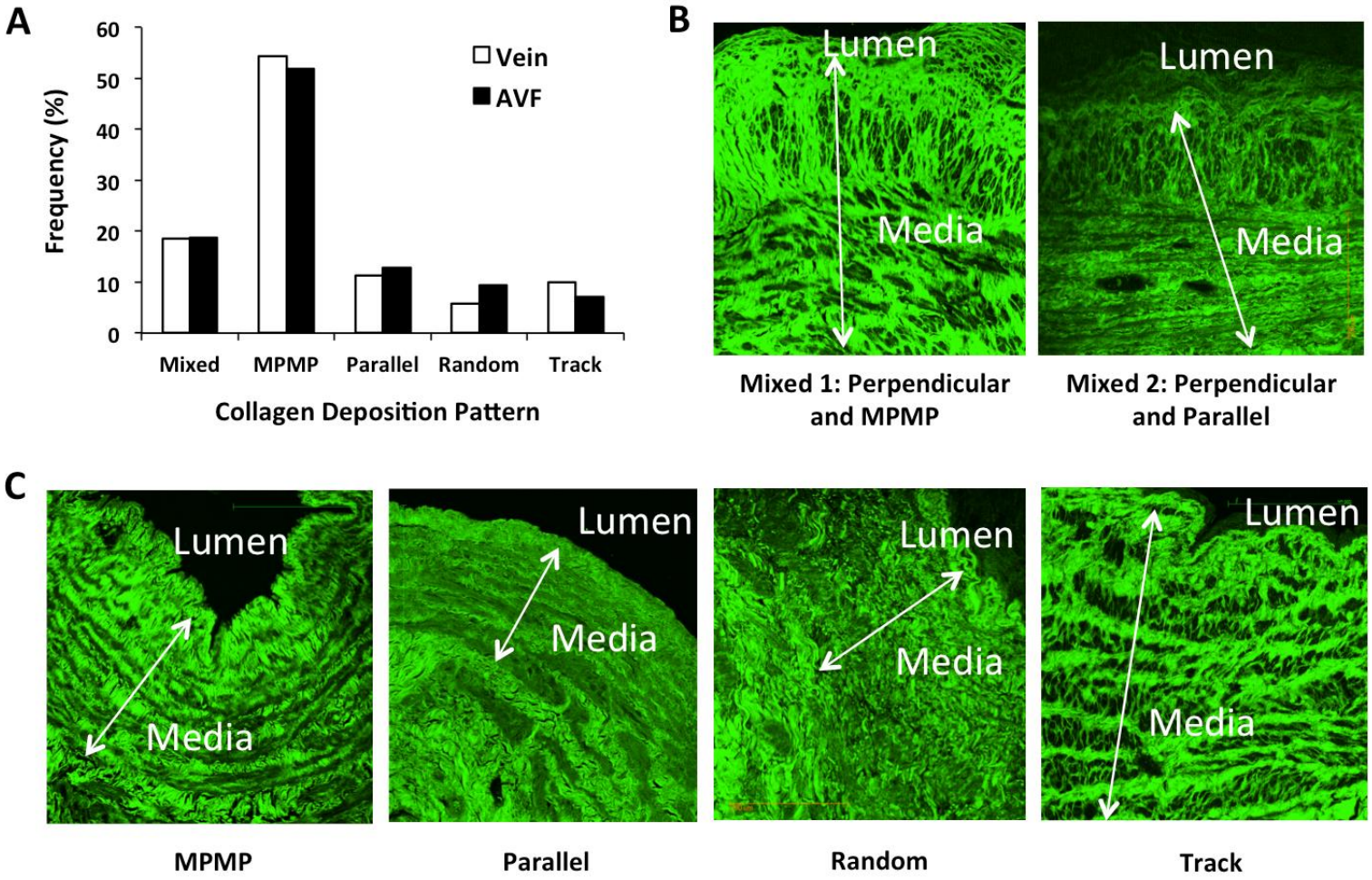

Supplemental Figure 7. Patterns of collagen deposition in the media of native veins (pre-existing) and AVFs (postoperative). A) Frequency of collagen deposition patterns in the first-stage (veins) and second-stage (AVFs) cohorts. **B-C)** Representative microphotographs of collagen deposition patterns. Abbreviations: MPMP, micro-perpendicular with macro-parallel.